frontiers in Energy Research

ORIGINAL RESEARCH
published: 15 October 2021
doi: 10.3389/fenrg.2021.725010

Energetics of Li^+ Coordination with Asymmetric Anions in Ionic Liquids by Density Functional Theory

Drace Penley[1], *Stephen P. Vicchio*[2], *Rachel B. Getman*[2] *and Burcu Gurkan*[1]*

[1]*Chemical and Biomolecular Engineering, Case Western Reserve University, Cleveland, OH, United States,* [2]*Chemical and Biomolecular Engineering, Clemson University, Clemson, SC, United States*

The energetics, coordination, and Raman vibrations of Li solvates in ionic liquid (IL) electrolytes are studied with density functional theory (DFT). Li^+ coordination with asymmetric anions of cyano(trifluoromethanesulfonyl)imide ([CTFSI]) and (fluorosulfonyl)(trifluoro-methanesulfonyl)imide ([FTFSI]) is examined in contrast to their symmetric analogs of bis(trifluoromethanesulfonyl)imide ([TFSI]), bis(fluorosulfonyl)imide ([FSI]), and dicyanamide ([DCA]). The dissociation energies that can be used to describe the solvation strength of Li^+ are calculated on the basis of the energetics of the individual components and the Li solvate. The calculated dissociation energies are found to be similar for Li^+-[FTFSI], Li^+-[TFSI], and Li^+-[FSI] where only Li^+-O coordination exists. Increase in asymmetry and anion size by fluorination on one side of the [TFSI] anion does not result in significant differences in the dissociation energies. On the other hand, with [CTFSI], both Li^+-O and Li^+-N coordination are present, and the Li solvate has smaller dissociation energy than the solvation by [DCA] alone, [TFSI] alone, or a 1:1 mixture of [DCA]/[TFSI] anions. This finding suggests that the Li^+ solvation can be weakened by asymmetric anions that promote competing coordination environments through enthalpic effects. Among the possible Li solvates of $(Li[CTFSI]_n)^{-(n-1)}$, where n = 1, 2, 3, or 4, $(Li[CTFSI]_2)^{-1}$ is found to be the most stable with both monodentate and bidentate bonding possibilities. Based on this study, we hypothesize that the partial solvation and weakened solvation energetics by asymmetric anions may increase structural heterogeneity and fluctuations in Li solvates in IL electrolytes. These effects may further promote the Li^+ hopping transport mechanism in concentrated and multicomponent IL electrolytes that is relevant to Li-ion batteries.

Keywords: ionic liquid electrolytes, lithium solvation, concentrated electrolytes, lithium-ion battery, *ab initio* thermodynamics

OPEN ACCESS

Edited by:
Ah-Hyung Alissa Park,
Columbia University, United States

Reviewed by:
Hailei Zhao,
University of Science and Technology Beijing, China
Shrihari Sankarasubramanian,
University of Texas at San Antonio, United States

***Correspondence:**
Burcu Gurkan
beg23@case.edu

Specialty section:
This article was submitted to Electrochemical Energy Conversion and Storage, a section of the journal Frontiers in Energy Research

Received: *14 June 2021*
Accepted: *10 September 2021*
Published: *15 October 2021*

Citation:
Penley D, Vicchio SP, Getman RB and Gurkan B (2021) Energetics of Li^+ Coordination with Asymmetric Anions in Ionic Liquids by Density Functional Theory. Front. Energy Res. 9:725010. doi: 10.3389/fenrg.2021.725010

INTRODUCTION

The structure of Li^+ solvates in concentrated electrolytes has a significant impact on Li^+ transport and is influential in the rate capability of rechargeable lithium ion batteries (LIBs) (Borodin et al., 2018; Yamada et al., 2019; Krachkovskiy et al., 2020; Pham et al., 2021). ILs present an extreme case of a concentrated electrolyte where the electrolyte is made entirely of discrete ions and lacks neutral solvent molecules. Generally, ILs are known to have high ionic conductivity, large electrochemical windows, and negligible volatility (Bae et al., 2013; Navarra, 2013). These properties are desirable for lithium battery systems and thus are of great interest for safe, high-density energy storage devices (Galinski et al., 2006; Bae et al., 2013; Navarra, 2013; Eftekhari et al., 2016). However, Li^+ transport in

ILs is complex and hindered by the high viscosity, mainly due to Coulombic interactions and specific Li^+–anion interactions, which leads to the formation of clusters that decrease the mobility of Li^+ in the bulk liquid (Lesch et al., 2014; Pham et al., 2021). Li^+ transport in ILs has been studied mostly by Raman spectroscopy, nuclear magnetic resonance spectroscopy, transference measurements, density functional theory (DFT), and classical molecular dynamic (MD) simulations (Borodin et al., 2006; Umebayashi et al., 2007; Duluard et al., 2008; Lassègues et al., 2009; Umebayashi et al., 2010; Castiglione et al., 2011; Fujii et al., 2013; Haskins et al., 2014; Borodin et al., 2018). In this study, the DFT approach is employed to understand the impact of anion asymmetry and the presence of binary anions on the structure and energetics of the first solvation shell of Li^+ in IL electrolytes.

The bis(trifluoromethanesulfonyl)imide, [TFSI], anion and its respective ILs have been widely studied as potential electrolytes for lithium metal batteries and LIBs, and were shown to improve battery performance over the state-of-the-art organic carbonate electrolytes with Li[PF_6] (Sakaebe and Matsumoto, 2003; Garcia et al., 2004; Armand et al., 2009). Fundamental studies of IL electrolytes with [TFSI] anion showed that Li^+ coordinates with anionic oxygen atoms where on average slightly less than four oxygen atoms are involved (Borodin et al., 2006), leading to two anions in the first solvation shell where *cis* conformation is favored with increased Li salt doping (Umebayashi et al., 2010). These studies were focused on Li salt mole fraction of x_{Li^+}<0.2. In the similar Li salt concentration range, Fujii et al. showed that in the case of [FSI], the solvation number increases to three anions in the first shell where both monodentate and bidentate bonds coexist (Fujii et al., 2013; Lesch et al., 2016). Later, Lesch et al. (2016) showed that when both [TFSI] and [FSI] anions are available, Li^+ prefers to coordinate with [TFSI] and forms Li^+-[TFSI]-Li^+ dimers which move on a similar timescale as Li^+-[TFSI] aggregates. Haskins et al. (2014) studied the Li^+ solvation and transport in pyrrolidinium ILs with [TFSI] and [FSI] anions, and imidazolium IL with tetrafluoroborate [BF_4] anion, with each system having 0.5 molal Li-salt concentration. When examining the solvation structures, they observed that the binding distances increased in the order of Li^+-[FSI] > Li^+-[TFSI] > Li^+-[BF_4], where the system with [BF_4] had the strongest binding energy and the system with [FSI] had the weakest binding energy. Different than previous studies, Haskins et al. reported that three [TFSI] anions coordinate with Li^+ through two monodentate and two bidentate bonds, while the coordination with [BF_4] and [FSI] involved four anions with each having monodentate binding. The differences from the previous reports were attributed to the higher Li salt concentrations in their study (x_{Li^+}~0.33) and difficulty in characterizing the coordination environment with experimental spectroscopy in the previous reports. At high Li salt concentrations, Li et al. (2012) also showed increased [TFSI] coordination with fewer bidentate and more monodentate bonds. Haskins et al. also studied the residence time of neighboring ions to Li^+ among other transport parameters, including Li^+ diffusivity and conductivity. The correlated ion motion that corresponds to the vehicular motion was decreased with increasing Li salt concentration, suggesting that Li^+ moves through the liquid by anion exchange. They concluded that the majority (60%) of the transport occurred *via* vehicular motion, while Li^+ hopping was found to gain more significance with large-sized anions and increased Li^+ concentration. Therefore, the promotion of the hopping mechanism *via* anion exchange is the key for enhanced Li^+ mobility in concentrated electrolytes such as ILs considering the limitations of the vehicular mobility in the presence of Li^+ aggregates at x_{Li^+} > 0.05 (Brinkkötter et al., 2018; McEldrew et al., 2021).

Decreasing the solvation strength and the lifetime of coordinated species in LIB electrolytes have been suggested to play an important role in improving Li^+ mobility. Borodin et al. (2017) demonstrated the promotion of Li^+ transport in concentrated electrolytes where nano-heterogeneity decouples cations from anion cages. In other examples where heterogeneity was achieved by simple mixtures, Li^+ solvation was shown to weaken in binary organic carbonate mixtures (Matsuda et al., 2002), and the solvation shell was found to be more rigid in cyclic carbonates than in their linear counterparts (Fulfer and Kuroda, 2016). Shim (2018) studied the solvation structure and dynamics of a mixture of ethylmethyl carbonate (EMC), dimethyl carbonate (DMC), and ethylene carbonate (EC) with the Li[PF_6] salt by MD simulations. They reported that as the EC concentration increased, the solvent fluctuations in Li solvates decreased due to the preferred coordination of Li^+ with EC and increased local density by the ring structure of EC, which was consistent with the reports by Yang et al. (2010). The decreased solvent fluctuations resulted in increased viscosity and reduced Li^+ diffusion. Similar to organic mixture electrolytes, mixtures of ILs have been studied to increase conductivity by Li solvate structural fluctuations and reduced solvation strength (Yang et al., 2010; Kerner et al., 2015; Huang et al., 2019a; Huang et al., 2019b; Chen and Forsyth, 2019).

IL mixtures with [TFSI]/[FSI] anions have been studied the most to date due to the superior electrochemical properties of ILs paired with these anions. The [DCA] anion has also garnered attention due to its lower viscosity and higher conductivity than [TFSI]- and [FSI]-based ILs. In a study by Yoon et al. (2013), the [DCA] anion paired with a pyrrolidinium cation in a Li|$LiFePO_4$ cell showed stable cycling at elevated temperatures. Huang et al. (2019b) showed by a combined Raman spectroscopy and MD simulations study that at x_{Li^+}<0.2, Li^+ coordinates on average with four [DCA] anions *via* monodentate bonds in a binary Li salt/IL mixture with [DCA] anion as well as a Li salt/IL/IL ternary mixture with [TFSI]/[DCA] anions. Using attenuated total reflectance far-ultraviolet and deep-ultraviolet spectroscopy, Imai et al. (2020) reported similar results for the first solvation shell of Li^+ in the Li salt/IL binary electrolyte with [DCA] anions. Huang et al. (2019b) also studied the ion pair lifetimes by MD and Li^+ transference by an experimental polarization method employed in Li-Li symmetrical cells. It was found that Li^+ coordination was not a strong function of the Li salt in the ternary mixture with [TFSI]/[DCA] anions, in contrast to Li-salt/IL binary electrolytes with [TFSI]. The ion pair lifetime of Li^+-[TFSI] decreased with increasing [TFSI] concentration in the ternary electrolyte. This result was attributed to Li^+ preferring to coordinate with [DCA] and the addition of the [TFSI] anion breaking down the rigid first solvation shell due to the weaker coordination bond.

TABLE 1 | Anions of interest with full name as well as an abbreviation used within the study.

Anion	Full name	Structure
[DCA]	Dicyanamide	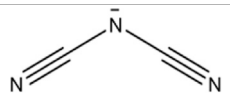
[CFSI]	Cyano(fluorosulfonyl)imide	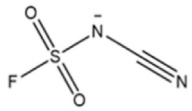
[CTFSI]	Cyano(trifluoromethanesulfonyl) imide	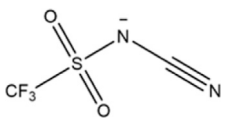
[FSI]	Bis(fluorosulfonyl)imide	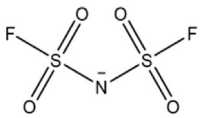
[TFSI]	Bis(trifluoromethanesulfonyl) imide	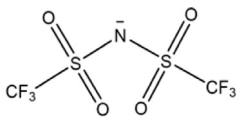
[FTFSI]	(fluorosulfonyl) (trifluoromethanesulfonyl) imide	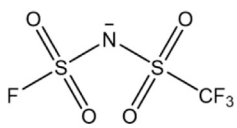
[PFTFSI]	(pentafluoroethanesulfonyl) (trifluoromethanesulfonyl)imide	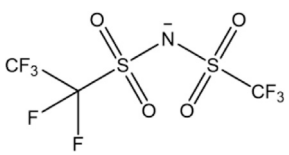
[HFTFSI]	(heptafluoropropanesulfonyl) (trifluoromethanesulfonyl)imide	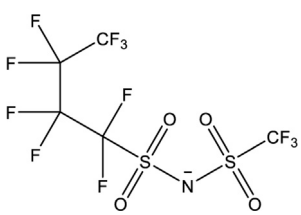

(Continued in next column)

TABLE 1 | (*Continued*) Anions of interest with full name as well as an abbreviation used within the study.

Anion	Full name	Structure
[NFFSI]	(nonafluorobutanesulfonyl) (fluorosulfonyl)imide	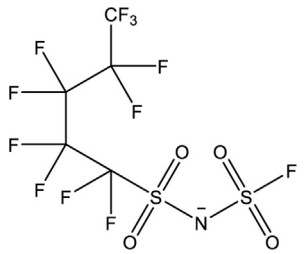
[NFTFSI]	(nonafluorobutanesulfonyl) (trifluoromethanesulfonyl) imide	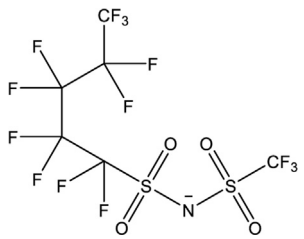

Very recently, Nurnberg et al. (2020) studied the Li^+ solvation and transport in IL electrolytes (x_{Li^+} = 0.1–0.7) with the [CTFSI] anion by Raman spectroscopy and pulsed gradient NMR measurements. This anion is an asymmetric analog to both [TFSI] and [DCA] anions. They found that the [CTFSI]-based electrolyte had lower conductivity than the [TFSI] system. However, a pronounced transition from vehicular to structural diffusion (hopping) was noted for the asymmetric anion. Studies on such asymmetric anions are scarce, and mixture anions in IL electrolytes are relatively recently being explored. Understanding the Li^+ coordination environments and the solvation energies in the case of asymmetric anions are important for tuning concentrated electrolytes for future energy storage devices. In this study, we calculated the optimized geometries, Raman vibrations, and the Li solvate energies by DFT to understand the effect of anion functionality in IL mixtures with Li salts. Several asymmetric anions based on [FSI], [TFSI], and [DCA] parent anions were studied and compared in terms of the anion size, extent of fluorination, and coordination chemistry. The structures of the studied anions as well as their abbreviation are listed in **Table 1**.

The bulk properties and electrochemical applications of the three asymmetric anions such as [NFTFSI], [CTFSI], and [FTFSI] are relatively unexplored when compared to their parent anions. The [CTFSI] anion in an IL electrolyte has shown promise in LIBs, with improved thermal and anodic stability, and exhibited higher room temperature conductivity than [DCA] and [TFSI] parent anions (Hoffknecht et al., 2017). However, the structure of the Li solvate was not studied, and it is not clear what the role of the liquid structure is on the improved performance. An investigation on the [FTFSI]-based IL electrolyte showed that

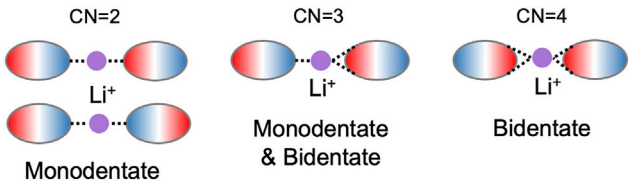

FIGURE 1 | Representative coordination environments for Li^+ with two asymmetric solvating anions forming bidentate and/or monodentate bonds. Li^+ is represented by the purple circle and the asymmetric anion is represented by the ovals, with red and blue color codes corresponding to the different coordination sites.

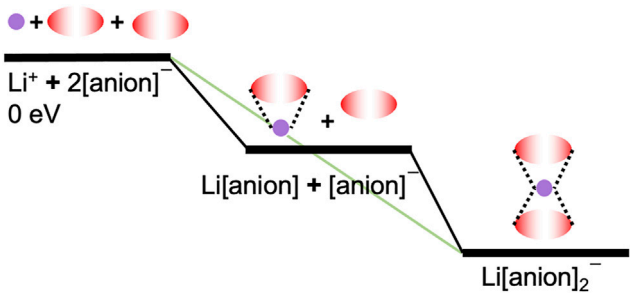

FIGURE 2 | Comparison of differential and integral analyses for Li solvates with a symmetrical anion. Bidentate binding is illustrated for one and two coordinating anions. Energy levels are indicated by the black horizontal bars where the starting individual components have 0 eV as a reference and the Li solvates have <0 eV. The differential energies are represented by the solid black lines and the integral energy is represented by the diagonal green line that connects the 0 eV state with the $Li[anion]_2^{-1}$ solvate at the lowest energy state.

the vehicular motion dominates due to the formation of Li^+ aggregates until 0.4 mole fraction of the Li salt after which the transport of Li^+ *via* hopping increases (Brinkkötter et al., 2018). [NFTFSI] is unique in that rather than combining the functionality of two parent IL anions, the fluoromethane group on [TFSI] is replaced with a fluorobutane. This provides the ability to quantify how the increased fluorination impacts the structure and transport properties. There has been little investigation of the [NFTFSI] and [NFFSI] anions in the past. Palumbo et al. (2017) studied the conformer structures of [NFTFSI] in a pyrrolidinium IL. Han et al. (2011) utilized 1M Li[NFFSI] as the conducting salt in organic carbonates (EC/EMC 3:7 v/v) to improve high temperature performance of LIBs. Li [NFFSI] showed similar conductivity as $Li[ClO_4]$ and slightly lower than $Li[PF_6]$; however, Li[NFFSI] did not corrode the aluminum current collector of the graphite/$LiCoO_2$ cell with 63% capacity retention over 100 cycles at 60°C, while the cell with $Li[PF_6]$ failed rapidly. Therefore, how the length of fluorination impacts the stability of LIBs is important to understand for extreme temperature conditions. In order to do so, we need a better understanding of how these fluorinated anions solvate and interact with Li^+ in the bulk electrolyte. The [CFSI], [PFTFSI], and [HFTFSI] anions were studied here to explore how the degree of fluorination of the asymmetric anions impacts solvation strength. Previously, it was found that the binding energies of Li solvates with organic ligands decreased with increased fluorination (Bauschlicher, 2018). It was also shown that with reduced dipole moment and an increased ligand size, the ligand–ligand repulsion was increased. This was discussed to possibly lead to different structures than the non-fluorinated analogs. In this study, we show how the strength of solvation is impacted by the asymmetry of the coordinating anions and how the anion mixtures compare to the analogous asymmetric anion that has binary coordination with Li^+. We report the strength of the first solvation shell of Li^+ in ILs without the impacts of the IL cation through DFT calculations and suggest which anions may help promote Li^+ transport based on this first principles study.

METHODS

Computational Details

Dissociation energies (E_D) were used to assess the thermodynamic favorabilities of the different Li^+-anion systems. E_D represents the amount of energy it takes to break Li^+-anion clusters into their constituents (i.e., the difference in energy going from the Li^+-anion cluster to the individual components of Li^+ and the anion at infinite separation). They were calculated using quantum mechanics in the absence of solvation, similar to a prior study on Li^+ transport in cross-linked polymer electrolytes with ILs (Elmore et al., 2018), according to the equation:

$$E_D = \left[E_{Li^+} + \sum_i y\,(E_{anion})_i\right] - E_{Li-solvate}, \quad (1)$$

where E_{Li}^+ is the electronic energy of the lithium ion, E_{anion} is the electronic energy of the isolated anion i, y is the number of anion i in the solvate structure, and $E_{Li\text{-}solvate}$ is the electronic energy of the Li solvate. In this study, $1 \le y \le 4$. The isolated Li^+ is modeled with a +1 charge, and each anion is modeled with a net charge of −1. The net charge of the Li solvate can hence be 0, −1, −2, and −3, depending on the number of coordinating anions. This analysis is limited to a maximum number of coordinating anions of four due to the repulsive forces between anions when the first solvation shell includes five anions or greater, resulting in concentrated environments of $0.20 \le x_{Li}^+ \le 0.50$. According to **Eq. 1**, positive values of E_D are favorable, with increasing values of E_D indicating stronger Li^+ ion bonds. Thus, a more positive E_D value is interpreted as a more stable Li solvate, and a more negative E_D value is interpreted as less stable, which would allow for faster breakdown of the first solvation shell and thus quicker exchange of anions within this shell.

Quantum mechanics calculations were carried out in the Gaussian 16 program (Frisch et al., 2016) using the three-parameter Becke model with the Lee–Yang–Par modification (B3LYP) (Lee et al., 1988) functional for exchange and correlation and the 6-311G(d,p) (Ditchfield et al., 1971) basis set. Structures of the isolated anions and Li^+ solvate systems and their associated electronic energies were obtained using geometry optimizations with default convergence criteria; as the Li^+ system does not require geometry optimization, its electronic energy was

calculated as a "single point." Frequency calculations were carried out at the same level of theory in order to obtain thermodynamic and Raman spectroscopic data. Raman frequencies were scaled by a factor of 0.964 (Palafox, 2018). An example Gaussian input file for a geometry optimization and frequency calculation is provided in the supplementary.

Coordination Number and Li Solvate Structures

It is important to note the distinction between the number of anions coordinating with Li^+ and the coordination number (CN) associated with this first solvation shell. An anion can have more than one bonding site for Li^+ in which case CN will be a greater number than the number of coordinating anions. For example, the *cis* and *trans* conformation of [TFSI] can yield bidentate and monodentate bonds which can result in CN of 1–4 as [TFSI] has four oxygen atoms that can coordinate with Li^+. **Figure 1** demonstrates the possible monodentate and bidentate binding with two coordinating anions. The represented anions are asymmetric as illustrated by the color code (blue and red). Thus, with two coordinating asymmetric anions, a CN of two, three, or four is possible.

Differential vs. Integral Analysis

Two methods were used to determine the energy difference associated with adding a new anion to the first solvation shell of Li^+. These methods can be visualized in **Figure 2** for a symmetric anion such as [TFSI] coordination with Li^+. The integral binding energy, which is equal to $-1 \times E_D$, is shown *via* the green diagonal line. It refers to the energy to add n anions to Li^+, for example, $Li^+ + 2[anion]^- \rightarrow Li[anion]_2^-$. In contrast, the differential binding energy is the energy to add one anion at a time, for example, $Li[anion] + [anion]^- \rightarrow Li[anion]_2^-$. The differential binding energy is useful for assessing the maximum number of anions that will coordinate to Li^+, whereas the integral binding energy is useful for assessing relative stabilities. A detailed example of the asymmetric [CTFSI] and [FTFSI] differential vs. integral analysis can be seen in **Supplementary Tables S1, S2**.

Ab Initio Thermodynamic Analysis

The thermodynamic stabilities of structurally and compositionally different Li solvates were calculated using an *ab initio* thermodynamic analysis (Soon et al., 2007; Getman et al., 2008; Grundner et al., 2015; Paolucci et al., 2016). This analysis was performed specifically for [TFSI]- and [DCA]-containing solvates. The *ab initio* thermodynamic analysis calculates the free energy of formation for different Li solvates at different mole fractions of [DCA] and [TFSI] in solution according to the following equation:

$$Li^+ + a[DCA] + b[TFSI] \overset{\Delta G}{\leftrightarrow} Li[DCA]_a[TFSI]_b, \quad (2)$$

where a is the number of [DCA] anions and b is the number of [TFSI] anions that coordinate to a single Li^+ cation. We used a library for the analysis that includes all [DCA]-only ($1 \le a \le 4$; $b = 0$), [TFSI]-only ($a = 0$; $1 \le b \le 3$), and [DCA]/[TFSI] ($1 \le a + b \le 3$) structures. According to the *ab initio* thermodynamic analysis, the free energy of formation for compositionally different structures ($Li[DCA]_a[TFSI]_b$) is calculated by transforming the free energy of a fixed number of species, $\Delta G(T, P, N_{Li^+}, N^*_{[TFSI]}, N^*_{[DCA]})$, where $*$ denotes that the anion species is coordinated with the Li^+ cation, to a fixed chemical potential using Legendre's transformations (see Supporting Information for more details). In this study, we transform $N^*_{[TFSI]}$ and $N^*_{[DCA]}$ to $\mu^*_{[TFSI]}$ and $\mu^*_{[DCA]}$; the resulting free energy of formation is denoted as $\Delta G^{(2)}$ (where the 2 superscript denotes two variables were transformed) and is given by the following equation:

$$\Delta G^{(2)}(T, P, N_{Li^+}, \mu^*_{TFSI}, \mu^*_{DCA}) = (\Delta E) - (\mu^*_{TFSI})(N^*_{TFSI}) - (\mu^*_{DCA}) \times (N^*_{DCA}), \quad (3)$$

where ΔE is the difference in electronic energy between a $Li[DCA]_a[TFSI]_b$ structure and the isolated Li^+ cation. Chemical potentials of [DCA] and [TFSI] are calculated (Starzak, 2010; Moučka et al., 2015) as follows:

$$\mu^*_i(T, x_i) = E_i + RTln(\gamma_i x_i), \quad (4)$$

where E_i is the electronic energy of the anion (i = DCA or TFSI), x_i is the mole fraction in solution, R is the gas constant, and γ_i is the activity coefficient. We assume a temperature of 298 K for all calculations and that all activity coefficients are equal to unity (Noda et al., 2001; Sun et al., 2018). The influence of this choice is detailed in the Supporting Information.

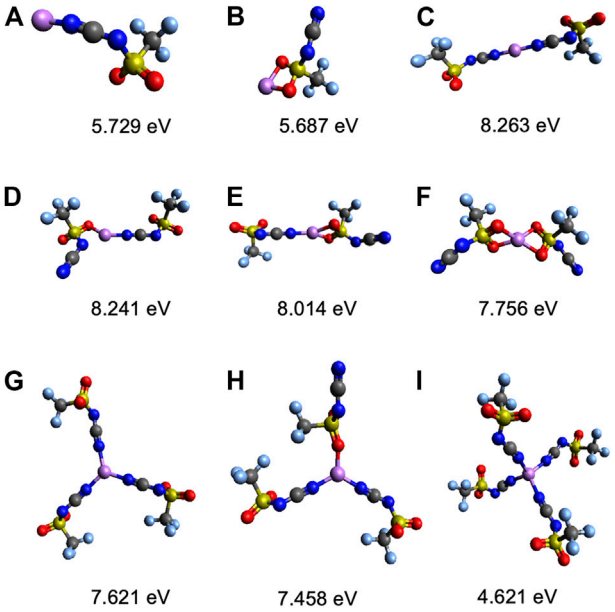

FIGURE 3 | Geometry optimized structures and calculated integral energies, E_D, of Li solvates with [CTFSI] for the number of coordinating anions of 1 **(A,B)**, 2 **(C–F)**, 3 **(G,H)**, and 4 **(I)**. The atom color code is as follows: red (oxygen), blue (nitrogen), yellow (sulfur), gray (carbon), purple (lithium), and light blue (fluorine).

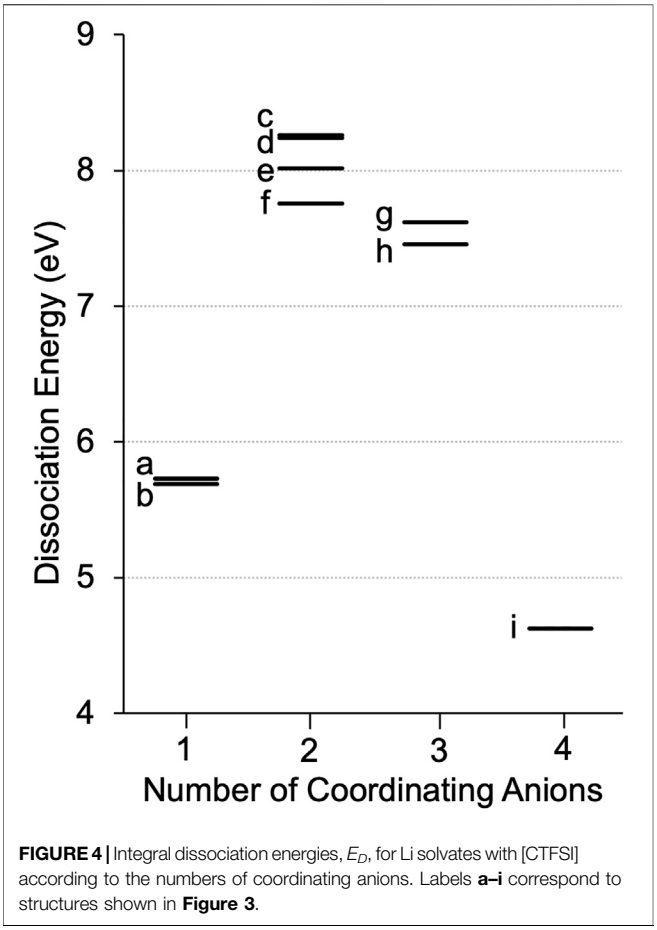

FIGURE 4 | Integral dissociation energies, E_D, for Li solvates with [CTFSI] according to the numbers of coordinating anions. Labels **a–i** correspond to structures shown in **Figure 3**.

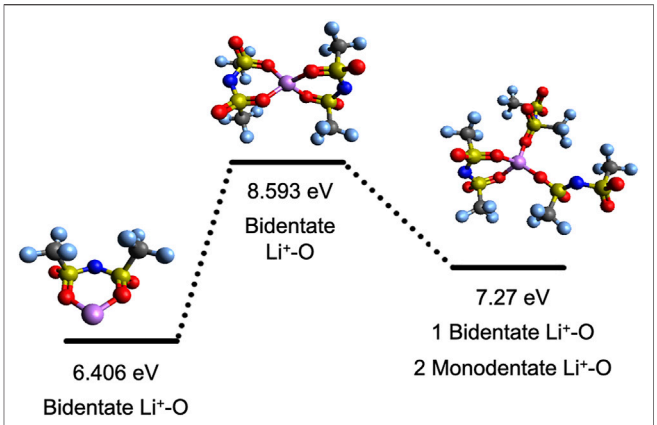

FIGURE 5 | Integral disassociation energies, E_D, and representative structures for Li^+-[TFSI] solvates with the respective coordination type. The color code for atoms is as follows: red (oxygen), blue (nitrogen), yellow (sulfur), gray (carbon), purple (lithium), and light blue (fluorine).

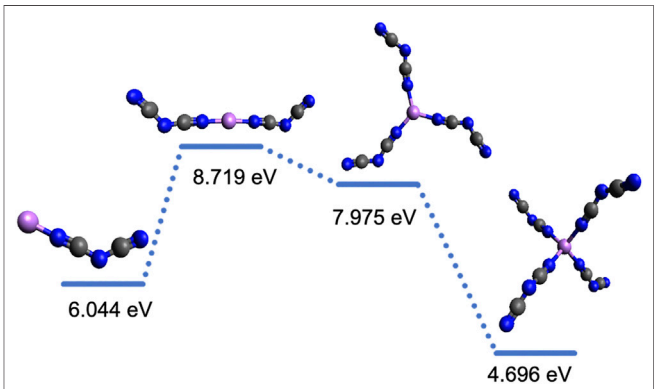

FIGURE 6 | Integral dissociation energies, E_D, and representative structures for Li^+-[DCA] systems with the respective coordination type (all monodentate Li^+-N). The color code for the atoms is as follows: blue (nitrogen), gray (carbon), and purple (lithium).

RESULTS AND DISCUSSION

Thermodynamically Favored Structure

The Li^+ solvation in the electrolyte is dynamic, and different populations of multiple solvate structures maybe present. In order to determine the most likely configurations, dissociation energies were calculated for all of the possible monodentate and bidentate coordination environments while incrementally increasing the number of anions around Li^+. The list of calculated E_D's for all of the Li solvates studied is in **Supplementary Table S3**. For the asymmetric [CTFSI], it is determined that Li^+ can coordinate with up to four anions where CN varies from one to four, as shown in **Figure 3**. Both the oxygen on the sulfonyl (Li^+-O) and the nitrogen on the cyano group (Li^+-N) can coordinate with Li^+. Therefore, when there is one [CFTSI] coordinating with Li^+, two configurations are possible, as seen in **Figures 3A,B**. With two coordinating anions, there are four possible configurations, as seen in **Figures 3C–F**. With three [CTFSI] anions, there are only two possible structures: all cyano coordination with monodentate bonds or two cyano and one sulfonyl oxygen coordination each with monodentate bonds, as shown in **Figures 3G,H**. Finally, moving to four coordinating anions, the only possible structure is seen in **Figure 3I** *via* monodentate Li^+-N bonds. The calculated E_D's for these Li solvate structures at differing numbers of coordinating anions are shown in **Figure 4**. It is interpreted that the structure with the highest E_D is the most stable since it requires more energy to break the coordination. Therefore, Li solvates with the highest E_D (strongest) among the multiple possible configurations for a specific coordination are said to be thermodynamically favored. According to the energies in **Figure 4**, for both Li[CTFSI] and $(Li[CTFSI]_2)^{-1}$, Li^+ prefers to coordinate with [CTFSI] *via* the cyano group (Li^+-N) over the sulfonyl oxygen atoms (Li^+-O). The most optimal Li solvate is $(Li[CTFSI]_2)^{-1}$ where Li^+ coordinates with two cyano groups each through monodentate conformation as in **Figure 3C** and/or one monodentate with cyano and another monodentate with sulfonyl, as in **Figure 3D**. Based on the three and four anion systems relying solely on Li^+-N coordination, all Li^+-N coordinated $(Li[CTFSI]_2)^{-1}$ are used for further analysis. This methodology for selecting the thermodynamically favored structures was implemented for all of the anions investigated in this study.

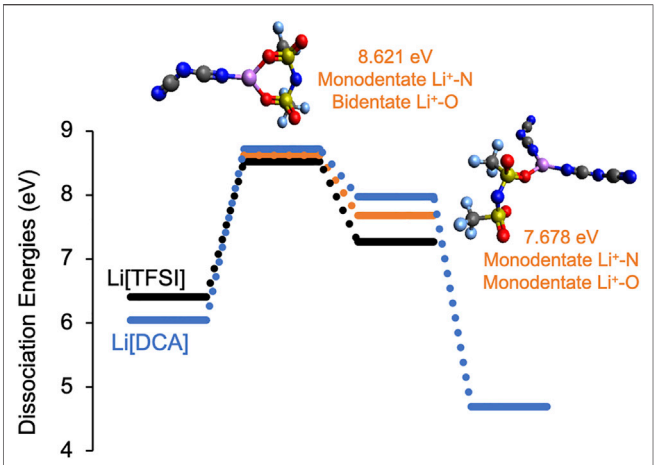

FIGURE 7 | Integral dissociation energies, E_D, and representative structures for Li solvates with [DCA]/[TFSI] anions (orange bars) in comparison to Li-[TFSI] (black bars) and Li-[DCA] (blue bars). The color code for the atoms is as follows: red (oxygen), blue (nitrogen), yellow (sulfur), gray (carbon), purple (lithium), and light blue (fluorine).

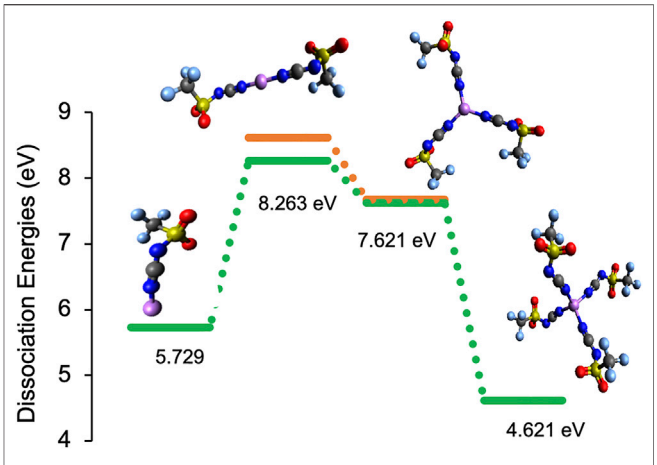

FIGURE 8 | Integral dissociation energies, E_D, and representative structures for Li-[CTFSI] solvates (green bars) in comparison to the Li-[DCA]/[TFSI] mixture (orange bars). All of the coordination environments are based on monodentate Li-N bonds. The color code for the atoms is as follows: red (oxygen), blue (nitrogen), yellow (sulfur), gray (carbon), purple (lithium), and light blue (fluorine).

To better understand the change in solvation energy with the asymmetric anion in comparison to the symmetric anions, the Li^+-[CTFSI] system was compared with the Li^+-[TFSI] and Li^+-[DCA] which are more widely studied experimentally (Sakaebe and Matsumoto, 2003; Garcia et al., 2004; Borgel et al., 2009; Yoon et al., 2013; Shen et al., 2015).

Further, the Raman frequencies of [TFSI], [DCA], and [CTFSI] with and without Li^+ coordination were calculated (spectra shown in **Supplementary Figures S1–S3**). The prominent vibrations were of the S-N-S and S=O bonds of [TFSI], and the C-N-C bond of [DCA]. For [CTFSI], the vibrations of interest are S-N-C_{CN}, S=O, and C≡N. With Li^+ coordination, the symmetric S-N-S stretch of *cis*-[TFSI] at 735 cm^{-1} experiences a blue shift by 10 cm^{-1}, which is consistent with previously reported experiments (Huang et al., 2019a; Huang et al., 2019b; Nurnberg et al., 2020). The S=O symmetric stretch appears at 1,132 and 1,148 cm^{-1}. With Li^+ coordination (structure in **Figure 5** with single [TFSI] coordinated to Li^+), the S=O peaks shift to 1,100 and 1,111 cm^{-1}. These vibrations have similar trends with [CTFSI]. Specifically, the S-N-C_{CN} peak in [CTFSI] at 762 cm^{-1} shifts to 779 cm^{-1} with Li^+ coordination (structure in **Figure 3B**). The S=O vibration of [CTFSI] at 1,118 cm^{-1} shifts to 1,099 cm^{-1}. Similarly, the C-N-C asymmetric and symmetric stretches of [DCA] at 2,183 and 2,199 cm^{-1} show blue shifts by 15 and 45 cm^{-1} (structure in **Figure 6** with single [DCA] coordinated to Li^+), respectively, which are also consistent with previous experimental findings (Huang et al., 2019b). [CTFSI] shows a similar peak location as [DCA] for the C≡N symmetric stretch at 2,195 cm^{-1}, with a blue shift of 42 cm^{-1} with Li^+ coordination (structure in **Figure 3A**), which is similar to the previous experimental findings (Nurnberg et al., 2020). The overall consistency of the peak locations and shifts when moving from the pure anion to the Li solvate provide confidence that our converged structures closely match with the known experimental reports.

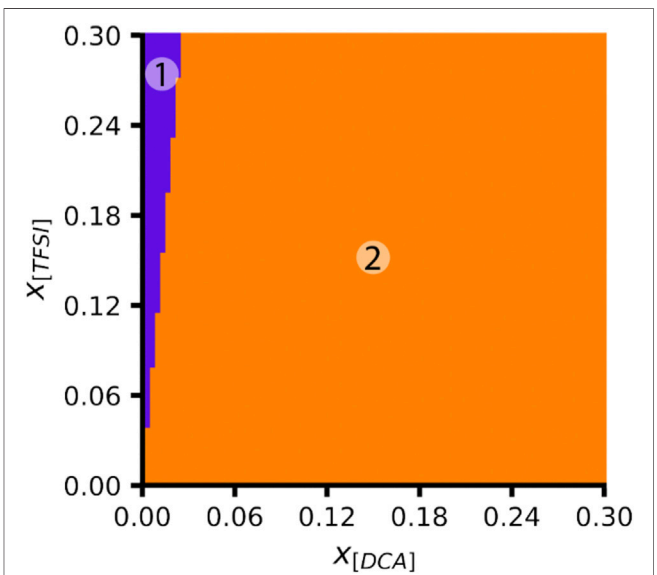

FIGURE 9 | Phase diagram for Li^+ solvates calculated in the *ab initio* thermodynamic analysis as a function of the mole fractions of [DCA] and [TFSI]. Color key: the purple region (1) = $(Li[TFSI]_2)^{-1}$ and the orange region (2) = $(Li[DCA]_2)^{-1}$.

Li^+ Solvation by [TFSI], [DCA], and [CTFSI]

Figures 5, **6** show the dissociation energies and structures for Li solvates with the [TFSI] and [DCA] anions, respectively. Li^+ has a CN of four with both [TFSI] and [DCA], according to the number of coordination sites. However, the number of anions in the first solvation shell for [TFSI] is three, while it is four for [DCA]. This is a result of [TFSI] coordination *via* the oxygen atoms on the same anion where the two Li^+-O coordination *via* bidentate bonds with two [TFSI] anions yield a CN of four, as seen in

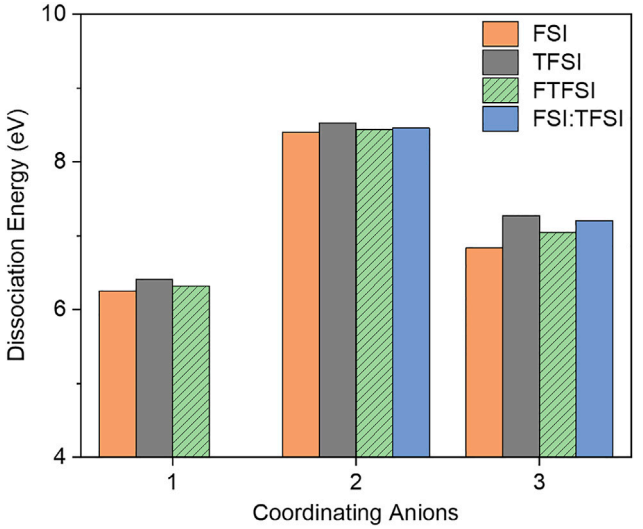

FIGURE 10 | Integral dissociation energies, E_D, of Li-[FSTFI] solvates in comparison to Li-[TFSI], Li-[FSI], and Li-[FSI]/[TFSI] mixture.

Figure 5. Previously, the integral binding energy for Li solvates with two [TFSI] anions calculated at the DFT/6-311+(d) level of theory was reported as −792.5 kJ/mol (8.2 eV) (Umebayashi et al., 2007), which is in reasonable agreement with our calculated Li $[TFSI]_2^{-1}$ (middle structure in **Figure 5**) E_D of 8.59 eV (828.8 kJ/mol). For [DCA], there is Li^+-N interaction *via* monodentate bonds; therefore, four [DCA] anions yield a CN of four, as seen in **Figure 6**. Based on these results, Li^+-N coordination is stronger than Li^+-O, especially when solvates with 2–3 anions are compared, which is consistent with previously reported results (Huang et al., 2019b). Therefore, one can suggest that Li solvates with a [DCA] anion will be more rigid, and this can hinder Li^+ hopping in comparison to Li solvates with [TFSI]. This is counterintuitive to the low viscosities that are promoted with [DCA] anion in ILs. It should be recalled that while smaller and more rigid Li solvates may have higher vehicular motion, the hopping mechanism can prevail at high Li salt concentrations with weaker solvate structures.

To further understand the relationship of how the differing anions affect the strength of the interaction between Li^+ and the [TFSI] and [DCA] anions, the E_D of the mixture system, [TFSI]/[DCA], as well as the individual anions are compared, as in **Figure 7**.

It should be noted that the minimum number of solvating anions for the [DCA]/[TFSI] system studied is two since a single anion would not capture the mixture behavior. Additionally, Li^+ solvation by three anions can either contain two [DCA] and one [TFSI] or *vice versa*; however, Li^+ coordination with two [DCA] anions provided a more thermodynamically favored structure (as shown in **Figure 7**). Comparing the Li^+ solvation energies of the [DCA]/[TFSI] mixture with those of [DCA]-only and [TFSI]-only systems, it is seen that with a CN of three, the mix-anion system (represented by orange bars in **Figure 7**) has a weaker E_D than Li-[DCA] (blue bars) and a stronger E_D than Li-[TFSI] (black) systems. For a perspective on how the mix-anion system of [DCA]/[TFSI] compares with the asymmetric analog of [CTFSI], the calculated dissociation energies are shown in **Figure 8**.

Based on the lower dissociation energies of Li solvates with the [CTFSI] anion, it can be said that the solvation cage is weakened by the anion asymmetry and the presence of competing coordination sites for Li^+. For example, comparing systems with two total solvation anions around Li^+, $(Li[CTFSI]_2)^{-1}$ has the most facile E_D of 8.26 eV in comparison to 8.59 eV for $(Li[TFSI]_2)^{-1}$, 8.62 eV for $(Li[DCA][TFSI])^{-1}$, and 8.72 eV for $(Li[DCA]_2)^{-1}$. When [CTFSI] was compared with a slightly different asymmetric anion [CFSI], similar results were obtained, where Li-[CFSI] has more facile E_D than the solvates with [FSI] or [DCA] alone. Further, Li-[CFSI] solvates had slightly reduced E_D when compared to [CTFSI] (see **Supplementary Figure S4**). To understand the influence of solution composition on the Li^+ solvate, we performed an *ab initio* thermodynamic analysis of the mix-anion [DCA]/[TFSI] system. The thermodynamic stability for the anionic [DCA]/[TFSI] system as a function of [DCA] and [TFSI] mole fraction is presented in **Figure 9**. Indeed, these results indicate that $(Li[DCA]_2)^{-1}$ is thermodynamically most preferred except for very low mole fractions of [DCA], where $(Li[TFSI]_2)^{-1}$ is preferred. None of the mix-anion structures are thermodynamically preferred according to the *ab initio* thermodynamic analysis.

Taken together, the above analysis suggests that assestment of ion pair lifetimes and measurement of the Li^+ transport when solvated by asymmetric anions would be interesting and necessary to understand the transport mechanism as these

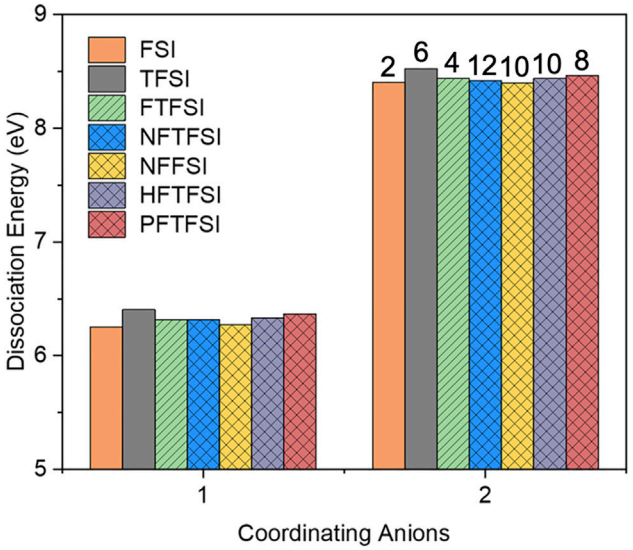

FIGURE 11 | Integral dissociation energies with respect to the number of coordinating asymmetric anions. [FTFSI] anion is highlighted with slashes, and all other asymmetric fluorinated anions are highlighted with crosshatches. PF, NF, and HF nomenclatures in front of TFSI or FSI stand for C_2F_5, C_3F_7, and C_4F_9 chains, respectively. The numbers on top of the bars indicate the number of total fluorines in the anion.

studies may provide a method to tune Li^+ hopping in concentrated electrolytes.

Li^+ solvation by [FSI], [TFSI], and [FTFSI]

Li solvates with the asymmetric anion [FTSFI] were also studied in comparison to [TFSI], [FSI], and the [FSI]/[TFSI] mixture. It has been shown that Li^+ transport is enhanced in ILs with [FSI]/[TFSI] mix-anions, resulting in improved battery cycling over the Li-IL binary mixtures with either the [FSI] or the [TFSI] anion (Lux et al., 2009; Bayley et al., 2011; Huang et al., 2019a). In order to understand whether the improvements in LIBs with these electrolytes originated from a change in solvation energies, we calculated the dissociation energies for this system, similar to the analysis performed for Li^+-[CTFSI]. **Figure 10** shows that the asymmetric [FTFSI] behaves similarly to [FSI] and the [FSI]/[TFSI] mixture. It should be noted that the Li solvate with the [FSI]/[TFSI] mixture and three coordinating anions consists of two [TFSI] and one [FSI], as this produced the more thermodynamically favored structure. The other configuration with two [FSI] and one [TFSI] system resulted in a dissociation energy of 6.907 eV, which is slightly lower than coordination with three [FTFSI] anions for $(Li^+\text{-}[FTFSI]_3)^{-2}$ at 7.045 eV. Unlike the [CTFSI] asymmetric anion, Li solvates with [FTFSI] have higher E_D than that of its parent anion [FSI], and the E_D of all configurations is similar. This is due to the single coordination chemistry through the sulfonyl oxygen in all of the cases considered in **Figure 10**. The most significant difference among Li solvates with [TFSI], [FSI], and [FTFSI] is that with three coordinating anions, [FSI] has all monodentate Li^+-O(=S) coordination, leading to a CN of three, while [FTFSI] and [TFSI] have one bidentate and two monodentate bonds, respectively, leading to a CN of four, as seen in **Supplementary Figure S5**. All other structures demonstrated bidentate configurations where CN was two for a single solvating anion and four for two solvating anions. Due to the similarities in the solvation structure, the only impact on the solvation strength comes from the fluorinated groups, either F-S ([FSI]) or CF_3-S ([TFSI] and [FTFSI]).

Fluorination Effects

The impacts of the length of fluorination and the degree of asymmetry on the calculated dissociation energies for Li solvates are captured in **Figure 11**. The asymmetry of the anions represented by the patterned bars in **Figure 11** is dictated by the length of the fluorinated alkyl chain on either the [FSI] or the [TFSI] parent anion. Specifically, the PF, NF, and HF nomenclatures in front of TFSI stand for C_2F_5, C_3F_7, and C_4F_9 chains, respectively, on the one side of the derivatized [TFSI] anion. As seen, there are no significant differences in E_D. The lowest dissociation energy is with [NFFSI] which has the longest fluorinated alkyl chains (C_4F_9) on the one side, with the other side being F-S.

While these results cannot point to a specific advantage of the longer fluorinated anions since they have the same enthalpic effects on Li^+ coordination, we expect to find entropic effects in solution which are not present in gas phase energy evaluations. In the case of [NFTFSI] and [NFFSI], the long fluorinated butane chains of each anion align with each other when the Li solvate has two anions with a CN of four *via* two bidentate bonds (**Supplementary Figure S6**). This alignment of the fluorinated alkyl chains may have a significant impact on the bulk liquid structure that cannot be evaluated by gas phase DFT calculations. We expect that the increase in the fluorination length will improve the viscosity and the solvation dynamics more than the enthalpic contributions to the dissociation energies, due to the delocalization of charge along the alkyl chain and inability of fluorochains solvating Li^+. In particular, the treatment of the entire system with IL cation and other cosolvents, if present, can provide more realistic solvate structures when longer chain fluorinated asymmetric anions are solvating Li^+. By studying these systems with MD simulations and experimental spectroscopic studies (Raman and NMR), the impact of fluorination on the bulk solvation and transport properties can be probed to a greater extent.

CONCLUSION

The solvation structure and energies of Li^+ with solvating anions of [TFSI], [DAC], [CTFSI], and [FTFSI] and a number of longer fluorinated anions with Li^+-O and Li^+-N coordination capability were calculated. The anions studied produced Li solvate structures with CNs of 2–4 depending on the size and functionality of the anion. Li solvates with a CN of two resulted in the highest dissociation energies (most stable conformers). Li solvates with a CN of one resulted in the lowest E_D with the exception of [DCA] and [CTFSI]. [DCA] and [CTFSI] were able to coordinate with four anions, and these Li solvates produced the lowest E_D (weakest). Through the E_D analysis, we found that the asymmetric [CTFSI] anion coordination with Li^+ is weaker than [TFSI] and [DCA] anions as well as the [TFSI]/[DCA] mixture. There are a larger number of solvate structures for Li-[CTFSI] solvate than those for [TFSI] and [DCA]. We suspect that this heterogeneity in the first solvation shell may lead to increased fluidity and structural diffusion (hopping) of Li^+ compared to solvates with [TFSI] and [DCA]. The [FTFSI] anion showed very similar results in terms of E_D as the [TFSI] and [FSI] parent anions due to the similar coordination environments between the three anions. However, [FTFSI] yielded slightly lower E_D than that of the Li^+ solvate with the parent anion mixture of [TFSI]/[FSI]. Given the weakened solvation energies, it would be interesting to study the impact of IL electrolytes with asymmetric anion on the Li^+ transference and performance of LIBs. The impact of fluorination length seems to have limited impact on E_D, with the longer fluorinated chains having slightly lower E_D than [TFSI]. However, we anticipate that these long fluorinated alkyl chains will have more significant entropic effects, which are not captured in gas phase DFT calculations. By studying these systems with MD simulations and experimental spectroscopic studies (Raman and NMR), the impact of fluorination on the bulk solvation and transport

properties can be probed to a greater extent. It will also be crucial for future studies to evaluate the impact of IL cations as well as the electric field present in Li batteries on the solvation structure and dynamics of Li^+.

DATA AVAILABILITY STATEMENT

The original contributions presented in the study are included in the article/**Supplementary Material**; further inquiries can be directed to the corresponding author.

AUTHOR CONTRIBUTIONS

DP performed the DFT calculations for geometries, vibrations, and dissociation energies. SV performed the *ab initio* thermodynamic analysis. RG supervised the *ab initio* thermodynamic analysis and contributed to the discussions. BG developed the plan, supervised DFT calculations, and contributed to the discussions. All authors contributed to the writing of the manuscript.

FUNDING

BG would like to acknowledge funding from the National Science Foundation (CBET, Award No. 1903259). BG and DP would also like to acknowledge the High Performance Computing Resource in the Core Facility for Advanced Research Computing at Case Western Reserve University. SV is supported by a GAANN Fellowship (Award Number: P200A180076) from the United States Department of Education.

SUPPLEMENTARY MATERIAL

The Supplementary Material for this article can be found online at: https://www.frontiersin.org/articles/10.3389/fenrg.2021.725010/full#supplementary-material

REFERENCES

Armand, M., Endres, F., MacFarlane, D. R., Ohno, H., and Scrosati, B. (2009). Ionic-Liquid Materials for the Electrochemical Challenges of the Future. *Nat. Mater.* 8 (8), 621–629. doi:10.1038/nmat2448

Bae, S.-Y., Shim, E.-G., and Kim, D.-W. (2013). Effect of Ionic Liquid as a Flame-Retarding Additive on the Cycling Performance and thermal Stability of Lithium-Ion Batteries. *J. Power Sourc.* 244, 266–271. doi:10.1016/j.jpowsour.2013.01.100

Bauschlicher, C. W. (2018). Li+-Ligand Binding Energies and the Effect of Ligand Fluorination on the Binding Energies. *Chem. Phys. Lett.* 694, 86–92. doi:10.1016/j.cplett.2018.01.047

Bayley, P. M., Best, A. S., MacFarlane, D. R., and Forsyth, M. (2011). Transport Properties and Phase Behaviour in Binary and Ternary Ionic Liquid Electrolyte Systems of Interest in Lithium Batteries. *ChemPhysChem* 12 (4), 823–827. doi:10.1002/cphc.201000909

Borgel, V., Markevich, E., Aurbach, D., Semrau, G., and Schmidt, M. (2009). On the Application of Ionic Liquids for Rechargeable Li Batteries: High Voltage Systems. *J. Power Sourc.* 189 (1), 331–336. doi:10.1016/j.jpowsour.2008.08.099

Borodin, O., Giffin, G. A., Moretti, A., Haskins, J. B., Lawson, J. W., Henderson, W. A., et al. (2018). Insights into the Structure and Transport of the Lithium, Sodium, Magnesium, and Zinc Bis(trifluoromethansulfonyl)imide Salts in Ionic Liquids. *J. Phys. Chem. C.* 122 (35), 20108–20121. doi:10.1021/acs.jpcc.8b05573

Borodin, O., Smith, G. D., and Henderson, W. (2006). Li+ Cation Environment, Transport, and Mechanical Properties of the LiTFSI Doped N-Methyl-N-alkylpyrrolidinium+TFSI- Ionic Liquids. *J. Phys. Chem. B.* 110 (34), 16879–16886. doi:10.1021/jp061930t

Borodin, O., Suo, L., Gobet, M., Ren, X., Wang, F., Faraone, A., et al. (2017). Liquid Structure with Nano-Heterogeneity Promotes Cationic Transport in Concentrated Electrolytes. *ACS Nano* 11 (10), 10462–10471. doi:10.1021/acsnano.7b05664

Brinkkötter, M., Giffin, G. A., Moretti, A., Jeong, S., Passerini, S., and Schönhoff, M. (2018). Relevance of Ion Clusters for Li Transport at Elevated Salt Concentrations in [Pyr12O1][FTFSI] Ionic Liquid-Based Electrolytes. *Chem. Commun.* 54, 4278–4281. doi:10.1039/C8CC01416G

Castiglione, F., Ragg, E., Mele, A., Appetecchi, G. B., Montanino, M., and Passerini, S. (2011). Molecular Environment and Enhanced Diffusivity of Li+ Ions in Lithium-Salt-Doped Ionic Liquid Electrolytes. *J. Phys. Chem. Lett.* 2 (3), 153–157. doi:10.1021/jz101516c

Chen, F., and Forsyth, M. (2019). Computational Investigation of Mixed Anion Effect on Lithium Coordination and Transport in Salt Concentrated Ionic Liquid Electrolytes. *J. Phys. Chem. Lett.* 10 (23), 7414–7420. doi:10.1021/acs.jpclett.9b02416

Ditchfield, R., Hehre, W. J., and Pople, J. A. (1971). Self-Consistent Molecular-Orbital Methods. IX. An Extended Gaussian-Type Basis for Molecular-Orbital Studies of Organic Molecules. *J. Chem. Phys.* 54 (2), 724. doi:10.1063/1.1674902

Duluard, S., Grondin, J., Bruneel, J.-L., Pianet, I., Grélard, A., Campet, G., et al. (2008). Lithium Solvation and Diffusion in the 1-Butyl-3-Methylimidazolium Bis(trifluoromethanesulfonyl)imide Ionic Liquid. *J. Raman Spectrosc.* 39 (5), 627–632. doi:10.1002/jrs.1896

Eftekhari, A., Liu, Y., and Chen, P. (2016). Different Roles of Ionic Liquids in Lithium Batteries. *J. Power Sourc.* 334, 221–239. doi:10.1016/j.jpowsour.2016.10.025

Elmore, C., Seidler, M., Ford, H., Merrill, L., Upadhyay, S., Schneider, W., et al. (2018). Ion Transport in Solvent-free, Crosslinked, Single-Ion Conducting Polymer Electrolytes for Post-Lithium Ion Batteries. *Batteries* 4 (2), 28. doi:10.3390/batteries4020028

Frisch, M. J., Trucks, G. W., Schlegel, H. B., Scuseria, G. E., Robb, M. A., Cheeseman, J. R., et al. (2016). *Gaussian 16 Rev. C.01*. Wallingford, CT.

Fujii, K., Hamano, H., Doi, H., Song, X., Tsuzuki, S., Hayamizu, K., et al. (2013). Unusual Li+Ion Solvation Structure in Bis(fluorosulfonyl)amide Based Ionic Liquid. *J. Phys. Chem. C.* 117 (38), 19314–19324. doi:10.1021/jp4053264

Fulfer, K. D., and Kuroda, D. G. (2016). Solvation Structure and Dynamics of the Lithium Ion in Organic Carbonate-Based Electrolytes: A Time-dependent Infrared Spectroscopy Study. *J. Phys. Chem. C.* 120 (42), 24011–24022. doi:10.1021/acs.jpcc.6b08607

Galiński, M., Lewandowski, A., and Stępniak, I. (2006). Ionic Liquids as Electrolytes. *Electrochimica Acta.* 51 (26), 5567–5580. doi:10.1016/j.electacta.2006.03.016

Garcia, B., Lavallée, S., Perron, G., Michot, C., and Armand, M. (2004). Room Temperature Molten Salts as Lithium Battery Electrolyte. *Electrochim. Acta.* 49 (26), 4583–4588. doi:10.1016/j.electacta.2004.04.041

Getman, R. B., Xu, Y., and Schneider, W. F. (2008). Thermodynamics of Environment-dependent Oxygen Chemisorption on Pt(111). *J. Phys. Chem. C.* 112 (26), 9559–9572. doi:10.1021/jp800905a

Grundner, S., Markovits, M. A. C., Li, G., Tromp, M., Pidko, E. A., Hensen, E. J. M., et al. (2015). Single-site Trinuclear Copper Oxygen Clusters in Mordenite for Selective Conversion of Methane to Methanol. *Nat. Commun.* 6 (1), 7546. doi:10.1038/ncomms8546

Han, H., Guo, J., Zhang, D., Feng, S., Feng, W., Nie, J., et al. (2011). Lithium (Fluorosulfonyl)(nonafluorobutanesulfonyl)imide (LiFNFSI) as Conducting Salt to Improve the High-Temperature Resilience of Lithium-Ion Cells. *Electrochem. Commun.* 13 (3), 265–268. doi:10.1016/j.elecom.2010.12.030

Haskins, J. B., Bennett, W. R., Wu, J. J., Hernández, D. M., Borodin, O., Monk, J. D., et al. (2014). Computational and Experimental Investigation of Li-Doped Ionic

Liquid Electrolytes: [pyr14][TFSI], [pyr13][FSI], and [EMIM][BF4]. *J. Phys. Chem. B.* 118 (38), 11295–11309. doi:10.1021/jp5061705

Hoffknecht, J.-P., Drews, M., He, X., and Paillard, E. (2017). Investigation of the N -Butyl- N -Methyl Pyrrolidinium Trifluoromethanesulfonyl- N -cyanoamide (PYR 14 TFSAM) Ionic Liquid as Electrolyte for Li-Ion Battery. *Electrochim. Acta.* 250, 25–34. doi:10.1016/j.electacta.2017.08.020

Huang, Q., Lee, Y.-Y., and Gurkan, B. (2019a). Pyrrolidinium Ionic Liquid Electrolyte with Bis(trifluoromethylsulfonyl)imide and Bis(fluorosulfonyl) imide Anions: Lithium Solvation and Mobility, and Performance in Lithium Metal-Lithium Iron Phosphate Batteries. *Ind. Eng. Chem. Res.* 58, 22587–22597. doi:10.1021/acs.iecr.9b03202

Huang, Q., Lourenço, T. C., Costa, L. T., Zhang, Y., Maginn, E. J., and Gurkan, B. (2019b). Solvation Structure and Dynamics of Li+ in Ternary Ionic Liquid-Lithium Salt Electrolytes. *J. Phys. Chem. B.* 123 (2), 516–527. doi:10.1021/acs.jpcb.8b08859

Imai, M., Tanabe, I., Ikehata, A., Ozaki, Y., and Fukui, K.-i. (2020). Attenuated Total Reflectance Far-Ultraviolet and Deep-Ultraviolet Spectroscopy Analysis of the Electronic Structure of a Dicyanamide-Based Ionic Liquid with Li+. *Phys. Chem. Chem. Phys.* 22 (38), 21768–21775. doi:10.1039/D0CP03865B

Kerner, M., Plylahan, N., Scheers, J., and Johansson, P. (2015). Ionic Liquid Based Lithium Battery Electrolytes: Fundamental Benefits of Utilising Both TFSI and FSI Anions?. *Phys. Chem. Chem. Phys.* 17 (29), 19569–19581. doi:10.1039/C5CP01891A

Krachkovskiy, S., Dontigny, M., Rochon, S., Kim, C., Trudeau, M. L., and Zaghib, K. (2020). Determination of Binary Diffusivities in Concentrated Lithium Battery Electrolytes via NMR and Conductivity Measurements. *J. Phys. Chem. C.* 124 (45), 24624–24630. doi:10.1021/acs.jpcc.0c07383

Lassègues, J.-C., Grondin, J., Aupetit, C., and Johansson, P. (2009). Spectroscopic Identification of the Lithium Ion Transporting Species in LiTFSI-Doped Ionic Liquids. *J. Phys. Chem. A.* 113 (1), 305–314. doi:10.1021/jp806124w

Lee, C., Yang, W., and Parr, R. G. (1988). Development of the Colle-Salvetti Correlation-Energy Formula into a Functional of the Electron Density. *Phys. Rev. B.* 37 (2), 785–789. doi:10.1103/physrevb.37.785

Lesch, V., Jeremias, S., Moretti, A., Passerini, S., Heuer, A., and Borodin, O. (2014). A Combined Theoretical and Experimental Study of the Influence of Different Anion Ratios on Lithium Ion Dynamics in Ionic Liquids. *J. Phys. Chem. B.* 118 (26), 7367–7375. doi:10.1021/jp501075g

Lesch, V., Li, Z., Bedrov, D., Borodin, O., and Heuer, A. (2016). The Influence of Cations on Lithium Ion Coordination and Transport in Ionic Liquid Electrolytes: a MD Simulation Study. *Phys. Chem. Chem. Phys.* 18 (1), 382–392. doi:10.1039/C5CP05111H

Li, Z., Smith, G. D., and Bedrov, D. (2012). Li+ Solvation and Transport Properties in Ionic Liquid/Lithium Salt Mixtures: A Molecular Dynamics Simulation Study. *J. Phys. Chem. B.* 116 (42), 12801–12809. doi:10.1021/jp3052246

Lux, S. F., Schmuck, M., Appetecchi, G. B., Passerini, S., Winter, M., and Balducci, A. (2009). Lithium Insertion in Graphite from Ternary Ionic Liquid-Lithium Salt Electrolytes: II. Evaluation of Specific Capacity and Cycling Efficiency and Stability at Room Temperature. *J. Power Sourc.* 192 (2), 606–611. doi:10.1016/j.jpowsour.2009.02.066

Matsuda, Y., Fukushima, T., Hashimoto, H., and Arakawa, R. (2002). Solvation of Lithium Ions in Mixed Organic Electrolyte Solutions by Electrospray Ionization Mass Spectroscopy. *J. Electrochem. Soc.* 149 (8), A1045. doi:10.1149/1.1489687

McEldrew, M., Goodwin, Z. A. H., Bi, S., Kornyshev, A. A., and Bazant, M. Z. (2021). Ion Clusters and Networks in Water-In-Salt Electrolytes. *J. Electrochem. Soc.* 168 (5), 050514. doi:10.1149/1945-7111/abf975

Moučka, F., Nezbeda, I., and Smith, W. R. (2015). Chemical Potentials, Activity Coefficients, and Solubility in Aqueous NaCl Solutions: Prediction by Polarizable Force Fields. *J. Chem. Theor. Comput.* 11 (4), 1756–1764. doi:10.1021/acs.jctc.5b00018

Navarra, M. A. (2013). Ionic Liquids as Safe Electrolyte Components for Li-Metal and Li-Ion Batteries. *MRS Bull.* 38 (7), 548–553. doi:10.1557/mrs.2013.152

Noda, A., Hayamizu, K., and Watanabe, M. (2001). Pulsed-Gradient Spin−Echo1H and19F NMR Ionic Diffusion Coefficient, Viscosity, and Ionic Conductivity of Non-chloroaluminate Room-Temperature Ionic Liquids. *J. Phys. Chem. B.* 105 (20), 4603–4610. doi:10.1021/jp004132q

Nürnberg, P., Lozinskaya, E. I., Shaplov, A. S., and Schönhoff, M. (2020). Li Coordination of a Novel Asymmetric Anion in Ionic Liquid-In-Li Salt Electrolytes. *J. Phys. Chem. B.* 124 (5), 861–870. doi:10.1021/acs.jpcb.9b11051

Palafox, M. A. (2018). DFT Computations on Vibrational Spectra: Scaling Procedures to Improve the Wavenumbers. *Phys. Sci. Rev.* 3 (6), 1–30. doi:10.1515/psr-2017-0184

Palumbo, O., Trequattrini, F., Appetecchi, G., and Paolone, A. (2017). A Study of the Conformers of the (Nonafluorobutanesulfonyl)imide Ion by Means of Infrared Spectroscopy and Density Functional Theory (DFT) Calculations. *Challenges* 8 (1), 7. doi:10.3390/challe8010007

Paolucci, C., Parekh, A. A., Khurana, I., Di Iorio, J. R., Li, H., Albarracin Caballero, J. D., et al. (2016). Catalysis in a Cage: Condition-dependent Speciation and Dynamics of Exchanged Cu Cations in SSZ-13 Zeolites. *J. Am. Chem. Soc.* 138 (18), 6028–6048. doi:10.1021/jacs.6b02651

Pham, T. D., Bin Faheem, A., Chun, S. Y., Rho, J. R., Kwak, K., and Lee, K. K. (2021). Synergistic Effects on Lithium Metal Batteries by Preferential Ionic Interactions in Concentrated Bisalt Electrolytes. *Adv. Energ. Mater.* 11 (11), 2003520. doi:10.1002/aenm.202003520

Sakaebe, H., and Matsumoto, H. (2003). N-Methyl-N-propylpiperidinium Bis(trifluoromethanesulfonyl)imide (PP13-TFSI) - Novel Electrolyte Base for Li Battery. *Electrochem. Commun.* 5 (7), 594–598. doi:10.1016/s1388-2481(03)00137-1

Shen, S., Fang, S., Qu, L., Luo, D., Yang, L., and Hirano, S.-i. (2015). Low-viscosity Ether-Functionalized Pyrazolium Ionic Liquids Based on Dicyanamide Anions: Properties and Application as Electrolytes for Lithium Metal Batteries. *RSC Adv.* 5 (114), 93888–93899. doi:10.1039/C5RA17539A

Shim, Y. (2018). Computer Simulation Study of the Solvation of Lithium Ions in Ternary Mixed Carbonate Electrolytes: Free Energetics, Dynamics, and Ion Transport. *Phys. Chem. Chem. Phys.* 20 (45), 28649–28657. doi:10.1039/C8CP05190A

Soon, A., Todorova, M., Delley, B., and Stampfl, C. (2007). Surface Oxides of the Oxygen-Copper System: Precursors to the Bulk Oxide Phase?. *Surf. Sci.* 601 (24), 5809–5813. doi:10.1016/j.susc.2007.06.062

Starzak, M. E. (2010). *Energy and Entropy*. New York, NY: Springer-Verlag.

Sun, Y., Xin, N., and Prausnitz, J. M. (2018). Solubilities of Five Lithium Salts in 1-Butyl-3-Methylimidazolium Dicyanamide and in 1-Butyl-3-Methylimidazolium Tetrafluoroborate from 298.15 to 343.15 K. *J. Chem. Eng. Data.* 63 (12), 4524–4531. doi:10.1021/acs.jced.8b00618

Umebayashi, Y., Mitsugi, T., Fukuda, S., Fujimori, T., Fujii, K., Kanzaki, R., et al. (2007). Lithium Ion Solvation in Room-Temperature Ionic Liquids Involving Bis(trifluoromethanesulfonyl) Imide Anion Studied by Raman Spectroscopy and DFT Calculations. *J. Phys. Chem. B.* 111 (45), 13028–13032. doi:10.1021/jp076869m

Umebayashi, Y., Mori, S., Fujii, K., Tsuzuki, S., Seki, S., Hayamizu, K., et al. (2010). Raman Spectroscopic Studies and *Ab Initio* Calculations on Conformational Isomerism of 1-Butyl-3-Methylimidazolium Bis-(trifluoromethanesulfonyl) amide Solvated to a Lithium Ion in Ionic Liquids: Effects of the Second Solvation Sphere of the Lithium Ion. *J. Phys. Chem. B.* 114 (19), 6513–6521. doi:10.1021/jp100898h

Yamada, Y., Wang, J., Ko, S., Watanabe, E., and Yamada, A. (2019). Advances and Issues in Developing Salt-Concentrated Battery Electrolytes. *Nat. Energ.* 4 (4), 269–280. doi:10.1038/s41560-019-0336-z

Yang, L., Xiao, A., and Lucht, B. L. (2010). Investigation of Solvation in Lithium Ion Battery Electrolytes by NMR Spectroscopy. *J. Mol. Liquids.* 154 (2), 131–133. doi:10.1016/j.molliq.2010.04.025

Yoon, H., Lane, G. H., Shekibi, Y., Howlett, P. C., Forsyth, M., Best, A. S., et al. (2013). Lithium Electrochemistry and Cycling Behaviour of Ionic Liquids Using Cyano Based Anions. *Energy Environ. Sci.* 6 (3), 979–986. doi:10.1039/C3EE23753B

Conflict of Interest: The authors declare that the research was conducted in the absence of any commercial or financial relationships that could be construed as a potential conflict of interest.

Publisher's Note: All claims expressed in this article are solely those of the authors and do not necessarily represent those of their affiliated organizations, or those of the publisher, the editors, and the reviewers. Any product that may be evaluated in this article, or claim that may be made by its manufacturer, is not guaranteed or endorsed by the publisher.